*J. Biochem.* 2009;145(4)429–435
doi:10.1093/jb/mvn183

# Concerted Effects of Two Activator Modules on the Group I Ribozyme Reaction

**Yoshiya Ikawa[1,2], Tomoaki Shiohara[3], Shoji Ohuchi[4] and Tan Inoue[3,5,*]**

*[1]Department of Chemistry and Biochemistry, Graduate School of Engineering, Kyushu University, Fukuoka 819-0351; [2]PRESTO, Japan Science and Technology Agency; [3]Graduate School of Biostudies, Kyoto University, Kyoto 606-8502; [4]Department of Basic Medical Sciences, Institute of Medical Science, The University of Tokyo, Tokyo 108-8639; and [5]ICORP, Japan Science and Technology Agency, Japan*

Received November 17, 2008; accepted November 28, 2008; published online January 3, 2009

**Group I intron ribozymes have a modular architecture and structural elements essential for catalysis. The elements are located in the conserved modular domain P3–P7 that is stabilized by another conserved module, P4–P6. It has been reported that artificial modules can complement the function of the native P4–P6. To exploit the modular architecture of group I ribozyme, we have constructed a hybrid ribozyme by attaching an artificial activator module to the wild-type T4 *td* ribozyme. Kinetic analysis of the hybrid ribozyme revealed that the artificial module and P4–P6 have unusual positive and negative concerted effects in activating the ribozyme.**

**Key words: activator, group I, intron, modular engineering, ribozyme.**

Abbreviations: WT, Wild-type.

## INTRODUCTION

Functional, structural and phylogenetic studies have been performed on large ribozymes, such as group I and II self-splicing introns, RNase P and ribosomes (*1*). One important aspect of their structure is their modularity (*2–4*). The structural modular units of group I self-splicing intron ribozymes are the most extensively studied among the ribozymes (*2*, *5*).

Group I ribozymes consist of a highly conserved core region and variable peripheral regions (*2*, *5–9*). The active site resides in the conserved core, whereas peripheral sites wrap the core by forming long-range RNA–RNA interactions (*2*). Thus, the peripheral sites constitute 'RNA cages', which are responsible for stabilizing the active conformation of the core.

The conserved core region is composed of two modular domains, P3–P7 and P4–P6 (Fig. 1A), which are connected via several tertiary interactions. In the crystal structure of a catalytically active group I ribozyme from purple bacterium *Azoarcus* (*10*), the P3–P7 module was shown to organize the binding pocket for guanosine cofactor, which initiates the self-splicing reaction. The module also provides four hydrogen bonds to hold two $Mg^{2+}$ ions that directly interact with the scissile phosphate.

In contrast, the P4–P6 module is not directly involved in guanosine binding. This module provides one hydrogen bond to hold one of the two $Mg^{2+}$ ions contacting the scissile phosphate, suggesting that P3–P7 is more crucial than P4–P6 in catalysis. The importance of the P3–P7 module was supported by the results of biochemical analysis of the T4 *td* group I intron (Fig. 1A), in which a mutant ribozyme lacking the whole P4–P6 module (M1 mutant, Fig. 1B) was found to perform phosphoester transfer reactions the rate of which was $10^3$-fold slower than that of the wild-type ribozyme reaction but still $10^8$-fold faster than that of the background reaction (*7*). Thus, it is possible that the role of P4–P6 is to activate the ribozyme by stabilizing the P3–P7 module (*7*, *10*, *11*) as well as to partly stabilize the transition state (*12*, *13*). P4–P6 is also suggested to participate in coordinating the first and second steps of the splicing reaction (*7*, *11*, *14*).

To explore artificial evolution of the group I intron, we performed *in vitro* evolution to generate artificial modules that can compensate for the function of native P4–P6 (*15*, *16*). Several activator modules were isolated from 40 random nucleotides inserted at the L7.1, L8 or L9 region of the M1 mutant lacking P4–P6 (Fig. 1B). A module designated #2.1 inserted at L9 (the resulting ribozyme was designated Clone-2.1 in the original report, and renamed M1 + 2.1 in this article) was the strongest activator among those examined (Fig. 1E). The $k_{cat}/K_m$ value of the resulting ribozyme was 2.8-fold higher than that of the wild-type in the presence of 20 mM $Mg^{2+}$. The new module (module #2.1) presumably improves substrate binding by employing base pairing between its L9b loop and the S-1 substrate RNA (Fig. 2). The observation that $K_m$ of the M1 + 2.1 ribozyme was 14-fold lower than that of the wild-type in the ligation reaction (reverse reaction of the first step of self-splicing) supports this hypothesis (*15*). This finding prompted us to investigate modular engineering of the T4 *td* group I ribozyme by combining the distinct properties of natural and artificial activator modules. Here, we report the design and construction of a new ribozyme designated WT + 2.1 that is a hybrid of the wild-type and the M1 + 2.1. The WT + 2.1 (Fig. 1D) was expected to show catalytic activity ($k_{cat}/K_m$) comparable or superior to that of the wild-type or M1 + 2.1.

*To whom correspondence should be addressed. Tel: +81-75-753-3995; Fax: +81-75-753-3996; E-mail: tan@kuchem.kyoto-u.ac.jp

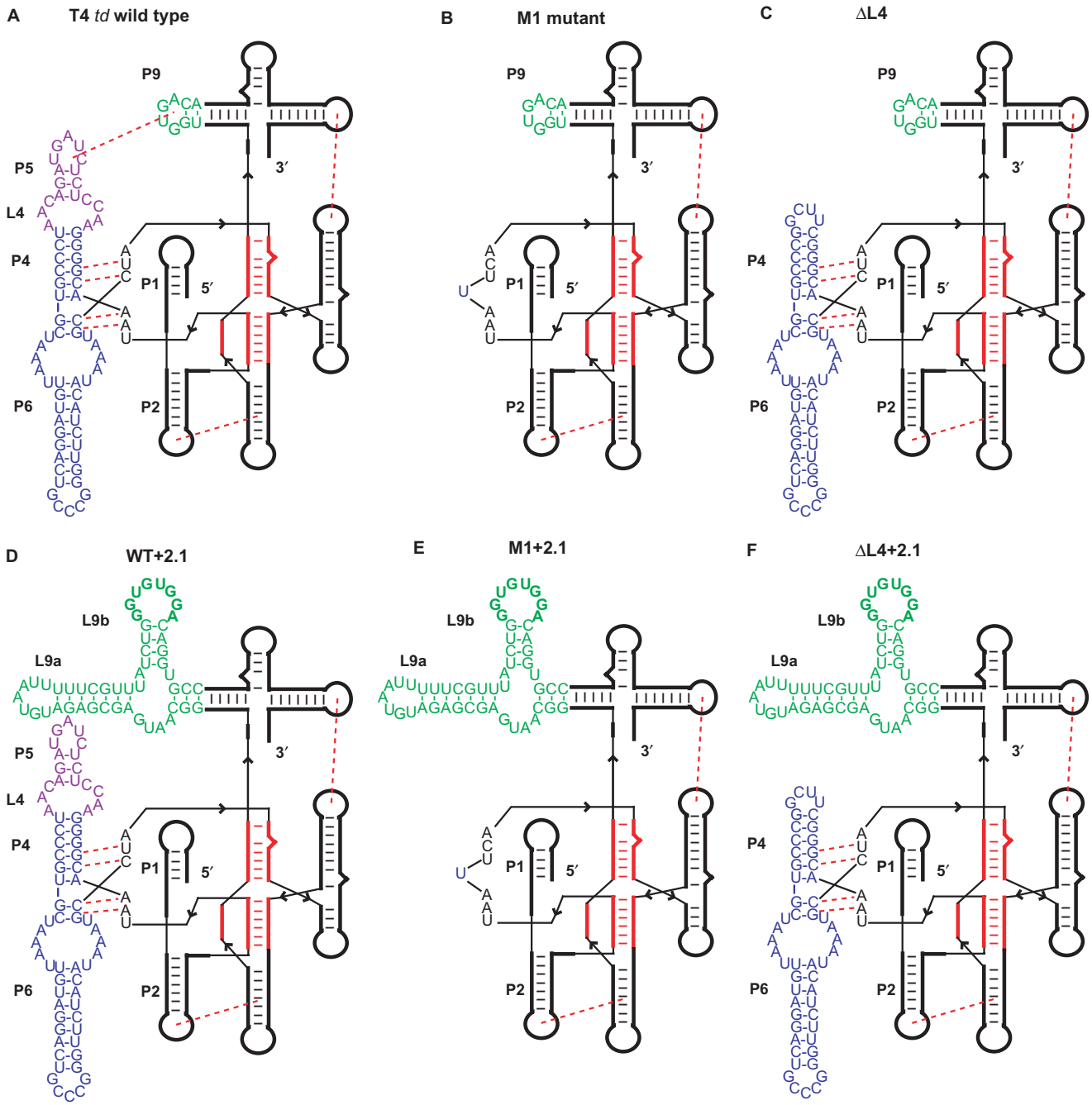


Fig. 1. **Secondary structure of the T4 td group I ribozyme and its derivatives.** Wild-type T4 td ribozyme (A). M1 mutant lacking the whole P4–P6 module (B). ΔL4 ribozyme. (C) WT + 2.1 hybrid ribozyme (D). M1 + 2.1 ribozyme (E). ΔL4 + 2.1 hybrid ribozyme (F). The P3-P7 domain is shown in red. The native P4–P6 module is shown in blue. The P9 region and artificial #2.1 module are shown in green. Red broken lines represent the tertiary interactions discussed in this study. In the #2.1 module, bold letters indicate the sequence complementary to the S-1 substrate RNA. Arrowheads indicate the 5′–3′ directionality of the RNA chains.

## MATERIALS AND METHODS

*Reagents*—The restriction enzyme *Bsa*I and T4 DNA ligase were purchased from New England Biolabs (Boston, MA) and Toyobo (Osaka, Japan), respectively. ExTaq DNA polymerase used for PCR in this study was purchased from Takara (Otsu, Japan). Synthetic DNA oligonucleotides were purchased from Hokkaido System Science (Sapporo, Japan). RNA oligonucleotides were purchased from Dharmacon (Lafayette, CO). [α-$^{32}$P]GTP was obtained from Perkin Elmer (Boston, MA). T7 RNA polymerase was overexpressed as polyhistidine-tagged recombinant protein in *Escherichia coli* BL21, and obtained by Ni-NTA affinity column purification (Amersham Biosciences, Buckinghamshire, UK).

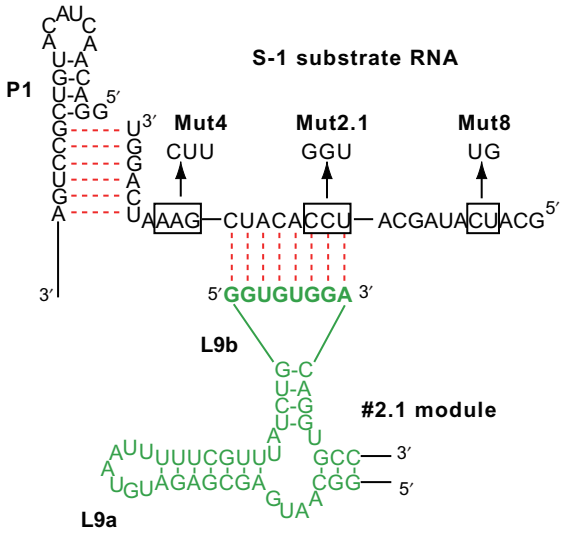


Fig. 2. **S-1 substrate and its interaction with #2.1 module.** Bold letters in the L9b loop region of the #2.1 module indicate the nucleotides forming base pairs with the S-1 substrate RNA. In the mutant substrate RNAs, boxed nucleotides in the S-1 RNA were substituted with the sequences indicated by arrows.

*Preparation of Plasmids*—Plasmids encoding hybrid ribozymes newly constructed in this study were derived from plasmids bearing the T4 *td* group I intron sequence (pTZtd) or its mutant derivatives. The plasmid encoding WT + 2.1 was constructed by inserting the #2.1 module into the T4 *td* intron sequence. Using pTZtd as a template, PCR was performed with the following pair of primers containing the sequence of the #2.1 module as well as a *Bsa*I site, 2.1-Fw: 5′-ACGGGCGGTCTCAGT AATTTTTCGTTTATCTGGGTGTGGACAGGTGCCTGCA GCTGGATATAATTCCGGGGTA-3′ and 2.1-Rev: 5′-ACG GGCGGTCTCATTACATCTCGCTCATTGCCTGCAGAGC AGACTATATCTCCAA-3′ (*Bsa*I site is underlined). The resulting PCR product was digested with *Bsa*I and self-ligated using T4 DNA ligase. Ligated DNA was transformed into *E. coli* JM109, and plasmids were isolated from the cultures. Sequences of isolated plasmids were verified by the dideoxy chain termination method using an ALF express II automated DNA sequencer (Amersham Pharmacia Biotech, Buckinghamshire, UK). Plasmids encoding M1 + 2.1 and ΔL4 + 2.1 were similarly constructed from plasmids encoding the M1 mutant and ΔL4, respectively.

*Preparation of Ribozymes*—All ribozymes used in this study were prepared by *in vitro* transcription using T7 RNA polymerase with [α-$^{32}$P]GTP (*17*). Template DNAs for *in vitro* transcription were amplified from plasmids bearing ribozymes by PCR with a set of primers Td-Fw 5′-*CTAATACGACTCACTATA*GGACAACTACATGTCGC CTGAGTATAAGGTGAC-3′ (the T7 promoter sequence is shown in italics) and Td-Rv 5′-ATTATGTTCAGATAAG GTCGTTAATC-3′. *In vitro* transcription reactions of ribozymes were performed at 37°C for 4 h, except for WT and WT + 2.1 that were performed at 30°C for 30 min to minimize self-cyclization of the ribozyme.

*Assay of Catalytic Efficiencies*—The efficiencies of the ligation reactions (the reverse of the first step of the self-splicing reaction) were assayed as follows. The ribozyme was dissolved in water to an appropriate final concentration as indicated in the figure legends and denatured at 70°C for 5 min, followed by 50°C for 5 min. The resulting RNA was folded at 50°C for 5 min by adding 10× reaction buffer followed by incubation at 37°C for 5 min. The reaction was started by adding the substrate RNA oligonucleotide. The final concentration of the reaction buffer was 50 mM Tris–Cl (pH 7.5), 2.5 mM spermidine, 5 or 20 mM $MgCl_2$, and the reaction mixtures were incubated at 37°C. At each time point, an aliquot was treated with an equal volume of stop solution consisting of 85% formamide, 100 mM EDTA and 0.1% xylene cyanol. Reaction products were separated by denaturing 5% polyacrylamide gel electrophoresis and quantified with a BAS-2500 Bio-Imaging Analyzer (Fuji Film, Tokyo, Japan). The data were plotted using Deltagraph 4.0 (Polaroid, Minnetonka, MN).

$k_{obs}$ was determined by fitting the data to the following equation:

$$\text{Fraction reacted} = a \times \exp(-k \times t) + b$$

where $t$ is time and $k$ is $k_{obs}$.

$k_{obs}$ was measured at four different substrate RNA concentrations. $K_m$ and $k_{cat}$ values were determined by plotting $1/k_{obs}$ to 1/[substrate]. All experiments were performed at least in duplicate.

## RESULTS

*Activity of the Hybrid Variant WT + 2.1*—We first examined the activity of the hybrid ribozyme (WT + 2.1) and its parental ribozymes (wild-type T4 *td* intron, M1 mutant lacking the P4–P6 module, and M1 + 2.1) in the presence of 5 or 20 mM $Mg^{2+}$ (Fig. 3A). The wild-type was active in the presence of 5 and 20 mM $Mg^{2+}$ (Fig. 3A). At 5 mM $Mg^{2+}$, the M1 + 2.1 ribozyme was active, whereas the activity of the M1 mutant was undetectable (Fig. 3A). Kinetic analyses indicated that the apparent product yield of the M1 + 2.1 was dependent on the concentration of the substrate RNA (Fig. 3B). As the substrate RNA bridges 5′ and 3′ regions of the M1 + 2.1 ribozyme, this observation suggested that the substrate RNA could act as a *trans*-activator or RNA chaperone that may induce and stabilize the active conformation of M1 + 2.1. The hybrid ribozyme (WT + 2.1) exhibited the highest product yield at both 5 and 20 mM $Mg^{2+}$ (Fig. 3A), suggesting that P4–P6 and #2.1 modules simultaneously enhanced the activity.

The M1 + 2.1 ribozyme forms base pairing between the #2.1 module and the original substrate (S-1) (*15*). To determine the importance of this base pairing in the WT + 2.1 ribozyme, we designed and employed three substrate RNAs (Fig. 2): one (mut-2.1) substrate with base substitutions that disrupt #2.1-substrate base pairing, while the remaining two (mut-4 and -8) have substitutions at positions outside the sites of base pairing. The activity of the wild-type was hardly dependent on the base substitutions of the substrate (Fig. 4B), whereas that of the M1 + 2.1 or hybrid ribozyme

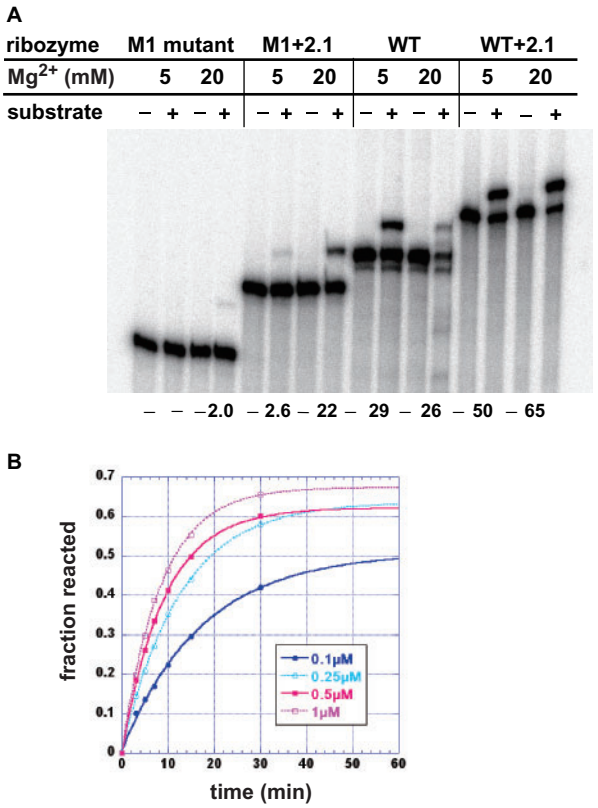


Fig. 3. **Effects of $Mg^{2+}$ ions on the ligation reactions.** (A) Ligation reaction of the ribozyme with 5 or 20 mM $Mg^{2+}$ ions. The reactions were performed with 2 nM ribozyme and 100 nM substrate RNA for 10 min at 37°C. Lower and upper bands correspond to the ribozymes and its self-ligated products, respectively. The product yields (%) are indicated at the bottom of each lane. (B) Time courses of the ligation reactions of the M1 + 2.1 ribozyme in the presence of various amounts of substrate RNA. Reactions were performed in the presence of 20 mM $Mg^{2+}$. Calculated final yields of the reactions were 0.50 (with 0.1 μM substrate), 0.63 (0.25 μM), 0.62 (0.5 μM) and 0.67 (1.0 μM).

(WT + 2.1) was markedly reduced in the reaction with the mut-2.1 substrate (Fig. 4A and B), indicating the importance of the base pairing for the ligation reaction of WT + 2.1.

*Kinetic Analysis for Ribozymes with #2.1 and P4–P6 Modules*—To understand the roles of P4–P6 and #2.1 modules in the ligation reaction, we determined the primary rate constant ($k_{cat}$) and Michaelis–Menten constant ($K_m$) of the wild-type and M1 + 2.1 in the presence of 5 mM $Mg^{2+}$, and compared the results with those in the presence of 20 mM $Mg^{2+}$ (Table 1) (*15*).

For the wild-type ribozyme, reduction of $Mg^{2+}$ ion concentration from 20 to 5 mM resulted in a marked decrease (31-fold) in $K_m$ value (5.5 and 0.18 μM at 20 and 5 mM $Mg^{2+}$, respectively). In the case of M1 + 2.1, however, reduction of $Mg^{2+}$ ion concentration caused only a modest decrease (3-fold) in $K_m$ value (0.4 and 0.13 μM at 20 and 5 mM $Mg^{2+}$, respectively). Thus, $Mg^{2+}$ ions had a 10-fold greater effect on the $K_m$ of the wild-type than that of M1 + 2.1 (Table 1). The higher $K_m$ value at 20 mM $Mg^{2+}$ may be due to misfolding of the T4 *td* ribozyme (*18*, *19*) resulting in deterioration of the substrate

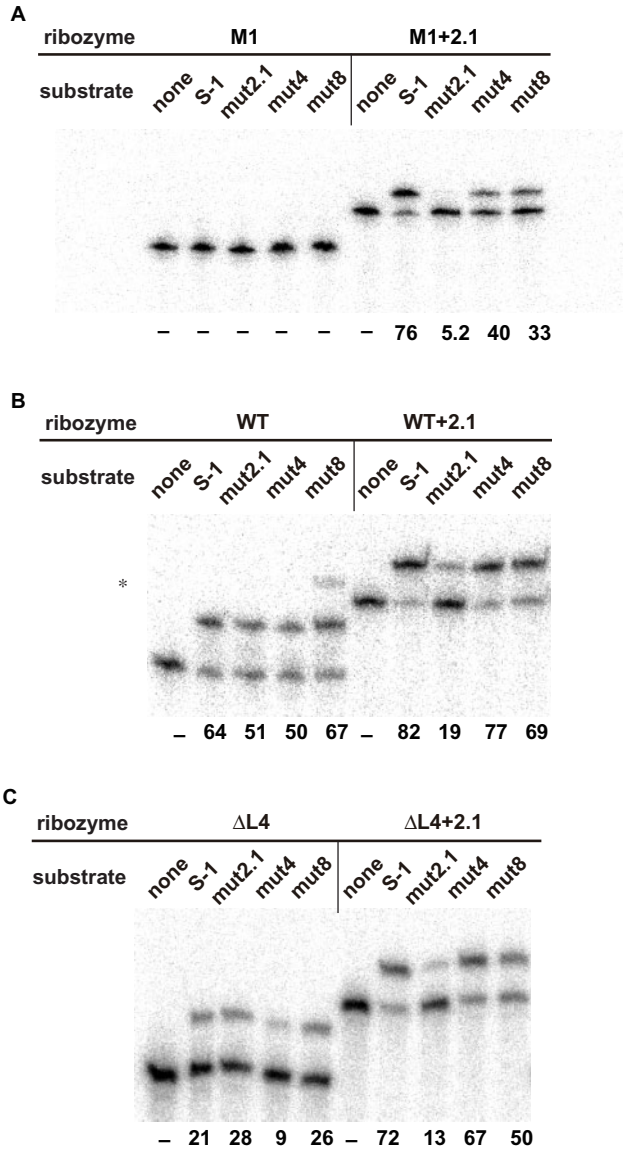


Fig. 4. **Ligation reactions of the ribozymes with different substrates.** (A) Ligation reaction of M1 mutant and M1 + 2.1 ribozyme with four substrate RNAs. Concentrations of the M1 mutant and M1 + 2.1 ribozyme were 230 nM and 170 nM, respectively. The reactions were performed with 500 nM substrate RNAs for 1 h at 37°C in the presence of 20 mM $Mg^{2+}$ ions. Lower and upper bands correspond to the ribozymes and the self-ligated products, respectively. The product yields (%) are indicated at the bottom of each lane. (B, C) Ligation reaction of the WT, WT + 2.1 (B) and ΔL4, ΔL4 + 2.1 (C) ribozyme with four substrate RNAs. The reactions were performed with 2 nM ribozyme except for WT with 3.5 nM ribozyme in the presence 500 nM substrate RNAs for 10 min at 37°C in the presence of 5 mM $Mg^{2+}$. Lower and upper bands correspond to the ribozymes and the self-ligated products, respectively. The product yields (%) are indicated at the bottom of each lane. The asterisk in Fig. 4B indicates an unidentified product, which was presumably an oligomer of ribozyme similar to that reported previously (*38*).

binding step. In contrast, reduction of $Mg^{2+}$ ion concentration showed weak effects on $k_{cat}$ values of the wild-type (1.2-fold decrease; 0.41 and 0.34 $min^{-1}$ at 20 and 5 mM $Mg^{2+}$, respectively) as well as those of the M1 + 2.1

Table 1. **Kinetic parameters.**

| Ribozyme | Substrate | $Mg^{2+}$ (mM) | $k_{cat}$ ($min^{-1}$) | $K_m$ (μM) | $k_{cat}/K_m$ ($min^{-1}/\mu M$) |
|---|---|---|---|---|---|
| T4 *td* wild-type[a] | S-1 | 5 | 0.34 | 0.18 | 1.8 |
| T4 *td* wild-type[a] | mut-2.1 | 5 | 0.41 | 0.39 | 1.1 |
| M1 + 2.1[a] | S-1 | 5 | 0.13 | 0.13 | 1.0 |
| M1 + 2.1[a] | mut-2.1 | 5 | ND[b] | ND[b] | ND[b] |
| WT + 2.1[a] | S-1 | 5 | 0.85 | 0.59 | 1.4 |
| WT + 2.1[a] | mut-2.1 | 5 | 0.09 | 1.0 | 0.09 |
| ΔL4[a] | S-1 | 5 | 0.06 | 0.12 | 0.5 |
| ΔL4 | mut-2.1 | 5 | 0.03 | 0.32 | 0.09 |
| ΔL4 + 2.1[a] | S-1 | 5 | 0.79 | 1.2 | 0.6 |
| ΔL4 + 2.1[a] | mut-2.1 | 5 | 0.02 | 3.25 | $6.2 \times 10^{-3}$ |
| M1[c] | S-1 | 20 | NA[d] | NA[d] | $2.1 \times 10^{-6}$ |
| T4 *td* wild-type[c] | S-1 | 20 | 0.41 | 5.5 | 0.075 |
| M1 + 2.1[c] | S-1 | 20 | 0.08 | 0.4 | 0.20 |
| M1 + 2.1[a] | mut-2.1 | 20 | NA[d] | NA[d] | $4.1 \times 10^{-4}$ |
| WT + 2.1 | S-1 | 20 | 0.90 | 1.7 | 0.53 |

[a]This study. [b]Not detectable. In the presence of 50 μM mut-2.1 substrate, ligated product was not detectable after reaction for 72 h. [c]Data from Ohuchi *et al.* (*15*). [d]Not available. Because of its high $K_m$ value (> 50 μM), $k_{cat}$ and $K_m$ values of the mutant were undetermined.

(1.6-fold increase: 0.08 and 0.13 $min^{-1}$ at 20 and 5 mM $Mg^{2+}$, respectively).

We next determined the kinetic parameters of the hybrid ribozyme (Table 1). In the presence of 5 mM $Mg^{2+}$, the $K_m$ value of WT + 2.1 (0.59 μM) was higher than those of M1 + 2.1 (0.13 μM) or WT (0.18 μM). Moreover, the $k_{cat}$ value of WT + 2.1 (0.85 $min^{-1}$) was also higher than those of the wild-type (0.34 $min^{-1}$) or M1 + 2.1 (0.13 $min^{-1}$). These results suggest that the coexistence of P4–P6 and #2.1 modules improved and reduced the rates of ligation and substrate binding, respectively, in the presence of 5 mM $Mg^{2+}$ ions. To determine the role of #2.1–substrate base pairing in the hybrid ribozyme, we examined the reaction with the mut-2.1 substrate incapable of base pairing with the #2.1 module (Table 1). The catalytic ability of WT + 2.1 with the mut-2.1 substrate ($k_{cat}/K_m = 0.09$) was 16-fold smaller than that of WT + 2.1 with the parental substrate ($k_{cat}/K_m = 1.4$). The inefficient reaction of the WT + 2.1 ribozyme with the mut-2.1 substrate was primarily due to reduction of $k_{cat}$ (9.4-fold) but not the increase of $K_m$ (1.7-fold) (Table 1). Thus, the catalytic properties of WT + 2.1 cannot be explained by simply summing the known roles of P4–P6 and the #2.1 module.

Biochemical, mutational and kinetic analyses of the #2.1 module have indicated that it primarily improves substrate binding by base pair formation (Table 1) (*15*). However, the function of the native P4–P6 module is more complex. In P4–P6, the P6 region primarily stabilizes the P3–P7 helices constituting the catalytic centre (*10*, *20–25*), whereas the L4 region, an internal loop conserved among all group I introns, interacts directly with the 5′ splice site (which was also the site of the ligation reaction in this study) (*10*, *3*, *26*). We determined the kinetic parameters of a mutant ribozyme lacking the L4 loop (ΔL4, Fig. 1C). In the reaction of ΔL4 mutant, $k_{cat}$ (0.06 $min^{-1}$) was 5.7-fold smaller than that of the wild-type (0.34 $min^{-1}$), whereas $K_m$ (0.12 μM) was comparable to that of the wild-type (0.18 μM). These observations were consistent with those of previous kinetic analyses of the *Tetrahymena* group I ribozyme. The L4 loop mainly assists transition state stabilization rather than docking of the P1 substrate helix in the *Tetrahymena* ribozyme (*13*, *27*).

To further investigate the effects of the P6 and L4 regions of the WT + 2.1 hybrid ribozyme, we removed the P5 and L4 regions from WT + 2.1. The resulting variant, ΔL4 + 2.1 (Fig. 1F), reacted poorly with the mut-2.1 substrate in comparison with the original S-1 substrate (Fig. 4C), indicating that the role of base pairing between the #2.1 module and the S-1 substrate (Fig. 2) is independent of that of the conserved L4 loop.

The $k_{cat}$ value of the ΔL4 mutant (0.06 $min^{-1}$) was improved by 13-fold with the #2.1 module ($k_{cat}$ of ΔL4 + 2.1 was 0.79 $min^{-1}$). The $k_{cat}$ value was much higher than that of the wild-type (0.34 $min^{-1}$) but comparable to that of the WT + 2.1 (0.85 $min^{-1}$) (Table 1). As observed in the WT + 2.1 ribozyme, addition of the #2.1 module negatively influenced substrate binding of the ΔL4 ribozyme (Table 1). These results indicated that the concerted effects of P4–P6 and #2.1 modules, which improved $k_{cat}$ value and deteriorated $K_m$ value, are not attributable to the P5 and L4 regions of P4–P6.

## DISCUSSION

*Kinetic Properties of the Hybrid Ribozyme*—In this study, the kinetic properties of a hybrid ribozyme (WT + 2.1) derived from T4 *td* group I ribozyme were investigated. WT + 2.1 contains an artificial #2.1 activator as an additional modular unit. If the #2.1 module by itself can activate the hybrid ribozyme, the reaction rate of WT + 2.1 should be comparable to that of the wild-type because the #2.1 module is much less involved in catalysis than the native P4–P6 (*15*). In addition, the substrate binding of the ribozyme is likely comparable with that of the M1 + 2.1 lacking P4–P6 because base pairing between substrate and #2.1 unit dominantly governs binding. However, the $k_{cat}$ of WT + 2.1 was 2.5-fold higher than that of the wild-type, whereas the $K_m$ of WT + 2.1 was 3.3-fold higher than that of M1 + 2.1 under the conditions employed in this study (Table 1). Interestingly, the data indicated unusual positive and negative synergism due to the two units, P4–P6 and #2.1. This may facilitate elucidation of a previously unknown aspect of the structural evolution of group I ribozymes.

*Possible Origin of the Improved $k_{cat}$ of the Hybrid Ribozyme*—Previous analyses of the T4 *td* group I ribozyme have suggested that the rate-limiting step of the reaction at the 5′ splice site is structural rearrangement of the P1–P2 substrate helices, which occurs significantly more slowly than the chemical step (*15*, *18*). This led to the hypothesis that deletion of the L4 loop should not affect $k_{cat}$ of ligation because the L4 loop primarily contributes to the chemical step (*13*). Consistent with this hypothesis, the improved $k_{cat}$ of the WT + 2.1 ribozyme does not depend on the L4 region because the $k_{cat}$ values of ΔL4 + 2.1 and WT + 2.1 were comparable (Table 1). Thus, it is possible that the

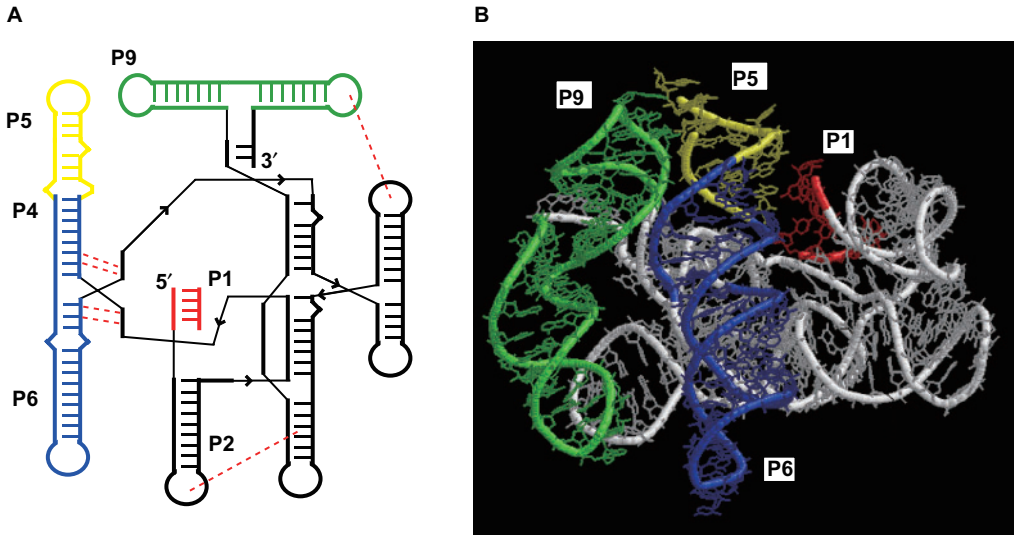


Fig. 5. **Structures of the Twort group I ribozyme.** (A) Secondary structure of a shortened Twort group I intron lacking the terminal loop of P1. The P1 helix is shown in red, and the P5 and P9 elements are shown in blue and green, respectively. Dashed red lines indicate tertiary interactions discussed in this study. Arrowheads indicate the 5′–3′ directionality of the RNA chain. (B) Three-dimensional (3D) structure of the Twort intron (*22*). Coloured regions in the 3D structure correspond to those in the secondary structure.

improved $k_{cat}$ value of the hybrid ribozyme is attributable to structural rearrangement of the substrate P1–P2 helices, and also to #2.1 and P4–P6 modules. Although the mechanism of this acceleration is currently unknown, it must involve the formation of #2.1–substrate base pairing because the $k_{cat}$ of WT + 2.1 with mut-2.1 substrate was significantly reduced (Table 1). The activity of ΔL4 + 2.1 also confirmed that P5 and L4 do not have a significant influence on the effect of #2.1. Thus, the improved $k_{cat}$ should be attributed to the P6 region in the hybrid ribozyme. The observations were consistent with the fact that the P3–P7 domain is fixed correctly via an interaction between P6 and P3 regions in the crystal structures of the *Azoarcus* and *Tetrahymena* group I ribozymes (*21*, *23*).

*Possible Origin of the Deteriorated* $K_m$ *Value of the Hybrid Ribozyme*—In the reactions of the WT + 2.1 and ΔL4 + 2.1, the $K_m$ values were higher than those of the parental ribozymes (wild-type, ΔL4 and M1 + 2.1), implying that the coexistence of P4–P6 and #2.1 negatively influences substrate binding. However, #2.1–substrate base pairing was not a primary determinant of $K_m$ for the hybrid ribozymes at 5 mM $Mg^{2+}$ because the difference in $K_m$ values of WT + 2.1 for the mut-2.1 substrate and original S-1 substrate (2.0-fold) was very close to those of the wild-type (2.2-fold) (Table 1).

The structure of the Twort group I intron ribozyme (*22*), a very close homologue of the T4 *td* intron, is useful for speculation on the relationship between P4–P6 and the #2.1 module in structural organization of T4 *td* intron ribozyme (Figs. 1A and 5). The terminal GUGA loop in P9 of the T4 *td* ribozymes was shown to interact with CU–AG pairs in the P5 region on the basis of the Twort intron structure combined with biochemical and phylogenetic analyses of the T4 phage introns (Figs. 1A and 5) (*28*, *29*). This leads to the suggestion that a physical conflict between P4–P6 and the #2.1 module extending from P9 may be involved in the unusual activity of the WT + 2.1 hybrid ribozyme.

*Implications for the Evolution of Ribozymes with Modular Architectures*—Naturally occurring large ribozymes often possess multiple activator modules. A typical example is the *Tetrahymena* group I intron ribozyme. Its peripheral elements, P5abc and P2-P2.1, have been shown to act as modular activators (*9*, *30–35*). P5abc and P2–P2.1, which are physically separable from the core of the intron ribozyme (*9*, *30*), appear to function collaboratively through intermodular base pairing (*2*). Further studies of the WT + 2.1 ribozyme and the *Tetrahymena* ribozyme that acquired two activators through natural evolution may provide a new tool for improving modular RNA engineering because they may reveal an unknown principle governing the natural evolutionary process (*35–37*).

## FUNDING

This work was partly supported by Grants-in-Aid for Young Scientists (A) (No.18685020 to Y.I.) and Exploratory Research (No.19657071 to Y.I.) from MEXT, Japan.

## CONFLICT OF INTEREST

None declared.

## REFERENCES

1. Gesteland, R.F., Cech, T.R., and Atkins, J.F. (2006) *The RNA World, Third Edition*, Cold Spring Habor Laboratory Press, Cold Spring Harbor, NY
2. Lehnert, V., Jaeger, L., Michel, F., and Westhof, E. (1996) New loop-loop tertiary interactions in self-splicing introns of subgroup IC and ID: a complete 3D model of the

*Tetrahymena thermophila* ribozyme. *Chem. Biol.* **12**, 993–1009
3. Massire, C., Jaeger, L., and Westhof, E. (1998) Derivation of the three-dimensional architecture of bacterial ribonuclease P RNAs from comparative sequence analysis. *J. Mol. Biol.* **279**, 773–793
4. Suzuki, T., Terasaki, M., Takemoto-Hori, C., Hanada, T., Ueda, T., Wada, A., and Watanabe, K. (2001) Structural compensation for the deficit of rRNA with proteins in the mammalian mitochondrial ribosome. Systematic analysis of protein components of the large ribosomal subunit from mammalian mitochondria. *J. Biol. Chem.* **276**, 21724–21736
5. Jaeger, L., Michel, F., and Westhof, E. (1996) The Structure of Group I Ribozymes in *Catalytic RNA* (Eckstein, F. and Lilley, D.M.J., eds.) pp. 33–51, Springer, Berlin
6. Beaudry, A.A. and Joyce, G.F. (1990) Minimum secondary structure requirements for catalytic activity of a self-splicing group I intron. *Biochemistry* **29**, 6534–6539
7. Ikawa, Y., Shiraishi, H., and Inoue, T. (2000) Minimal catalytic domain of a group I self-splicing intron RNA. *Nat. Struct. Biol.* **7**, 1032–1035
8. Ikawa, Y., Shiraishi, H., and Inoue, T. (2000) Characterization of P8 and J8/7 elements in the conserved core of the *Tetrahymena* group I intron ribozyme. *Biochem. Biophys. Res. Commun.* **267**, 85–90
9. Ikawa, Y., Shiraishi, H., and Inoue, T. (1998) *Trans*-activation of the *Tetrahymena* ribozyme by its P2-2.1 domains. *J. Biochem.* **123**, 528–533
10. Stahley, M.R. and Strobel, S.A. (2005) Structural evidence for a two-metal-ion mechanism of group I intron splicing. *Science* **309**, 1587–1590
11. Ikawa, Y., Yoshioka, W., Ohki, Y., Shiraishi, H., and Inoue, T. (2001) Self-splicing of the *Tetrahymena* group I ribozyme without conserved base-triples. *Genes Cells.* **6**, 411–420
12. Williams, K.P., Fujimoto, D.N., and Inoue, T. (1992) A region of group I introns that contains universally conserved residues but is not essential for self-splicing. *Proc. Natl Acad. Sci. USA.* **89**, 10400–10404
13. Strobel, S.A. and Ortoleva-Donnelly, L. (1999) A hydrogen-bonding triad stabilizes the chemical transition state of a group I ribozyme. *Chem. Biol.* **6**, 153–165
14. Tanner, M.A., Anderson, E.M., Gutell, R.R., and Cech, T.R. (1997) Mutagenesis and comparative sequence analysis of a base triple joining the two domains of group I ribozymes. *RNA* **3**, 1037–1051
15. Ohuchi, S.J., Ikawa, Y., Shiraishi, H., and Inoue, T. (2002) Modular engineering of a Group I intron ribozyme. *Nucleic Acids Res.* **30**, 3473–3478
16. Ohuchi, S.J., Ikawa, Y., Shiraishi, H., and Inoue, T. (2004) Artificial modules for enhancing rate constants of a Group I intron ribozyme without a P4-P6 core element. *J. Biol. Chem.* **279**, 540–546
17. Milligan, J.F., Groebe, D.R., Witherell, G.W., and Uhlenbeck, O.C. (1987) Oligoribonucleotide synthesis using T7 RNA polymerase and synthetic DNA templates. *Nucleic Acids Res.* **15**, 8783–8798
18. Pichler, A. and Schroeder, R. (2002) Folding problems of the 5′ splice site containing the P1 stem of the group I thymidylate synthase intron: substrate binding inhibition *in vitro* and mis-splicing *in vivo*. *J. Biol. Chem.* **277**, 17987–17993
19. Waldsich, C., Grossberger, R., and Schroeder, R. (2002) RNA chaperone StpA loosens interactions of the tertiary structure in the *td* group I intron *in vivo*. *Genes Dev.* **16**, 2300–2312
20. Adams, P.L., Stahley, M.R., Kosek, A.B., Wang, J., and Strobel, S.A. (2004) Crystal structure of a self-splicing group I intron with both exons. *Nature* **430**, 45–50
21. Adams, P.L., Stahley, M.R., Gill, M.L., Kosek, A.B., Wang, J., and Strobel, S.A. (2004) Crystal structure of a group I intron splicing intermediate. *RNA* **10**, 1867–1887
22. Golden, B.L., Kim, H., and Chase, E. (2005) Crystal structure of a phage Twort group I ribozyme-product complex. *Nat. Struct. Mol. Biol.* **12**, 82–89
23. Guo, F., Gooding, A.R., and Cech, T.R. (2004) Structure of the *Tetrahymena* ribozyme: base triple sandwich and metal ion at the active site. *Mol. Cell* **16**, 351–362
24. Vicens, Q. and Cech, T.R. (2006) Atomic level architecture of group I introns revealed. *Trends Biochem. Sci.* **31**, 41–51
25. Stahley, M.R. and Strobel, S.A. (2006) RNA splicing: group I intron crystal structures reveal the basis of splice site selection and metal ion catalysis. *Curr. Opin. Struct. Biol.* **16**, 319–326
26. Strobel, S.A., Ortoleva-Donnelly, L., Ryder, S.P., Cate, J.H., and Moncoeur, E. (1998) Complementary sets of noncanonical base pairs mediate RNA helix packing in the group I intron active site. *Nat. Struct. Biol.* **5**, 60–66
27. Szewczak, A.A., Ortoleva-Donnelly, L., Ryder, S.P., Moncoeur, E., and Strobel, S.A. (1998) A minor groove RNA triple helix within the catalytic core of a group I intron. *Nat. Struct. Biol.* **5**, 1037–1042
28. Jaeger, L., Michel, F., and Westhof, E. (1994) Involvement of a GNRA tetraloop in long-range RNA tertiary interactions. *J. Mol. Biol.* **236**, 1271–1276
29. Costa, M. and Michel, F. (1995) Frequent use of the same tertiary motif by self-folding RNAs. *EMBO J.* **14**, 1276–1285
30. van der Horst, G., Christian, A., and Inoue, T. (1991) Reconstitution of a group I intron self-splicing reaction with an activator RNA. *Proc. Natl Acad. Sci. USA.* **88**, 184–188
31. Doherty, E.A., Herschlag, D., and Doudna, J.A. (1999) Assembly of an exceptionally stable RNA tertiary interface in a group I ribozyme. *Biochemistry* **38**, 2982–2990
32. Russell, R. and Herschlag, D. (1999) New pathways in folding of the *Tetrahymena* group I RNA enzyme. *J. Mol. Biol.* **291**, 1155–1167
33. Engelhardt, M.A., Doherty, E.A., Knitt, D.S., Doudna, J.A., and Herschlag, D. (2000) The P5abc peripheral element facilitates preorganization of the *Tetrahymena* group I ribozyme for catalysis. *Biochemistry* **39**, 2639–2651
34. Johnson, T.H., Tijerina, P., Chadee, A.B., Herschlag, D., and Russell, R. (2005) Structural specificity conferred by a group I RNA peripheral element. *Proc. Natl Acad. Sci. USA.* **102**, 10176–10181
35. Ikawa, Y., Tsuda, K., Matsumura, S., and Inoue, T. (2004) *De novo* synthesis and development of an RNA enzyme. *Proc. Natl Acad. Sci. USA* **101**, 13750–13755
36. Ohuchi, S.P., Ikawa, Y., and Nakamura, Y. (2008) Selection of a novel class of RNA-RNA interaction motifs based on the ligase ribozyme with defined modular architecture. *Nucleic Acids Res.* **36**, 3600–3607
37. Saito, H. and Inoue, T. (2007) RNA and RNP as new molecular parts in synthetic biology. *J. Biotechnol.* **132**, 1–7
38. Wank, H. and Schroeder, R. (1996) Antibiotic-induced oligomerisation of group I intron RNA. *J. Mol. Biol.* **258**, 53–61